Journal of the Mechanical Behavior of Biomedical Materials 110 (2020) 103881

Contents lists available at ScienceDirect

Journal of the Mechanical Behavior of Biomedical Materials

journal homepage: http://www.elsevier.com/locate/jmbbm

Nonlinear stress-dependent recovery behavior of the intervertebral disc

Semih E. Bezci [a], Shiyin Lim [a], Grace D. O'Connell [a,b,*]

[a] Department of Mechanical Engineering, University of California, Berkeley, USA
[b] Department of Orthopaedic Surgery, University of California, San Francisco, USA

ARTICLE INFO

Keywords:
Intervertebral disc
Fluid flow
Recovery mechanics
Nonlinear viscoelasticity

ABSTRACT

The intervertebral disc exhibits complex mechanics due to its heterogeneous structure, inherent viscoelasticity, and interstitial fluid-matrix interactions. Sufficient fluid flow into the disc during low loading periods is important for maintaining mechanics and nutrient transport. However, there is a lack of knowledge on the effect of loading magnitude on time-dependent recovery behavior and the relative contribution of multiple recovery mechanisms during recovery. In most studies that have evaluated disc recovery behavior, a single load condition has been considered, making it difficult to compare findings across studies. Hence, the objective of this study was to quantify unloaded disc recovery behavior after compressive creep loading under a wide range of physiologically relevant stresses (0.2–2 MPa). First, the repeatability of disc recovery behavior was assessed. Once repeatable recovery behavior was confirmed, each motion segment was subject to three cycles of creep-recovery loading, where each cycle consisted of a 24-h creep at a pre-assigned load (100, 200, 300, 600, 900, or 1200 N), followed by an 18-h recovery period at a nominal load (10 N). Results showed that disc recovery behavior was strongly influenced by the magnitude of loading. The magnitude of instantaneous and time-dependent recovery deformations increased nonlinearly with an increase in compressive stress during creep. In conclusion, this study highlights that elastic deformation, intrinsic viscoelasticity, and poroelasticity all have substantial contributions to disc height recovery during low loading periods. However, their relative contributions to disc height recovery largely depend on the magnitude of loading. While loading history does not influence the contribution of the short-term recovery, the contribution of long-term recovery is highly sensitive to loading magnitude.

1. Introduction

The intervertebral disc provides spinal stability and mobility while sustaining large mechanical loads. Complex disc mechanics originate from its heterogeneous structure, inherent viscoelasticity, and interstitial fluid-matrix interactions (Cassidy et al., 1990; Costi et al., 2008; Hayes and Bodine, 1978). The disc consists of a gel-like nucleus pulposus surrounded by the annulus fibrosus, which has a multi-layered angle-ply structure. Despite differences in composition and structure, water is the primary constituent of both tissues (>65% by dry weight) (Antoniou et al., 1996; Iatridis et al., 2007) Moreover, the water content fluctuates by 15–25% during a diurnal cycle, with region-dependent differences in water loss (Botsford et al., 1994; Martin et al., 2018; McMillan et al., 1996). Disc mechanical properties are sensitive to hydration, which is altered by changes in tissue porosity, proteoglycan content, or osmotic differential between the tissue and surrounding environment (Bezci et al., 2015). Furthermore, load-induced fluid flow enhances the transport of large solutes through the disc (Ferguson et al., 2004; Urban et al., 1982). Thus, maintaining sufficient fluid flow into the disc during low loading periods is essential for maintaining healthy disc function and cell viability.

Measurable changes in disc height during diurnal loading or signal intensity of magnetic resonance images provide an indirect measure of intradiscal fluid movement (Martin et al., 2018). Mechanically, the disc responds to changes in load by undergoing an instantaneous elastic deformation followed by a time-dependent deformation (Kazarian, 1975). Previous *in vitro* studies used various empirical models to describe time-dependent deformation under creep, stress relaxation, and recovery (Bezci and O'Connell, 2018; Burns et al., 1984; Johannessen et al., 2004; Keller et al., 1990, 1987; MacLean et al., 2007; O'Connell et al., 2011; Riches et al., 2002; Van der Veen et al., 2013; Vergroesen et al., 2018). Although rheological models simplify complex deformations into one-dimensional measurements, they have been useful for evaluating the effects of loading history, hydration, injury, and degeneration on time-dependent behavior (Bezci and O'Connell, 2018; Burns et al., 1984; Campana et al., 2011; Cassidy et al., 1990; Hult et al.,

* Corresponding author. University of California, Berkeley Department of Mechanical Engineering, 5122 Etcheverry Hall, #1740, Berkeley, CA, 94720, USA.
E-mail address: g.oconnell@berkeley.edu (G.D. O'Connell).

https://doi.org/10.1016/j.jmbbm.2020.103881
Received 2 December 2019; Received in revised form 22 April 2020; Accepted 23 May 2020
Available online 30 May 2020

1995; Johannessen et al., 2004; Keller et al., 1990, 1988; 1987; Martin et al., 2013; O'Connell et al., 2011; Pollintine et al., 2010; Vergroesen et al., 2018).

Mechanical loading forces water out of the disc during loading. However, fluid flow into the disc during bed rest or low-loading recovery is partially driven by the osmotic difference between the tissue and surrounding environment (Bezci and O'Connell, 2018). As a result, time-dependent deformations in creep occur at a different rate than recovery (MacLean et al., 2007). Recovery tests are often performed under a nominal load to mimic bed rest recovery, which is predicted to be near 0.06 MPa for human discs (~100 N for L4L5 human discs) (Dreischarf et al., 2016; Ferguson et al., 2004; O'Connell et al., 2007; Schmidt et al., 2016a; Vergroesen et al., 2014; Wilke et al., 1999). Recently, osmotic loading has been used to drive fluid flow in glycosaminoglycan-rich tissues without altering the applied load (Kelly et al., 2013; Vergroesen et al., 2016). Our previous work showed that recovery in a hyperosmotic environment (*i.e.*, 1.5 M saline or 10× standard concentration) resulted in a shift in fluid flow during unloaded recovery (Bezci and O'Connell, 2018). During recovery in the hyperosmotic environment, fluid flow switched from flowing into the disc, which was noted by an increase in disc height, to flowing out of the disc (observed as a decrease in disc height).

To date, most studies refer to apparent time-dependent behavior as viscoelasticity, although time-dependent disc mechanics have contributions from both inherent fluid-independent viscoelasticity and fluid-dependent poroelasticity (Bezci and O'Connell, 2018). Inherent viscoelasticity is often associated with stretching and sliding motion of collagen fibrils, while poroelasticity is attributed to the flow of mobile water through the porous tissue matrix (Argoubi and Shirazi-Adl, 1996; Oftadeh et al., 2018; Xu et al., 2013). Previous studies suggested that poroelasticity dominates disc mechanics at long time scales, while viscoelastic effects are present at short time scales, providing partial recovery of disc height within minutes of unloading before poroelastic effects come into play (Bezci and O'Connell, 2018; Hsieh et al., 2005; Lu and Hutton, 1998; Vergroesen et al., 2016). This observation has also been noted for other biological tissues, such as brain and articular cartilage (Budday et al., 2017; DiSilvestro et al., 2001; Suh and Disilvestro, 1999; Zhu et al., 1993).

The magnitude of compressive stress applied to the disc varies in magnitude with changes in body posture, body weight, muscle activity, and external loads (Callaghan et al., 1998; Han et al., 2013; Nachemson, 1981; Wilke et al., 1999). For example, stresses on the disc while lifting an object in forward flexed posture are up to four times greater than the stress experienced during standing (Nachemson, 1981; Wilke et al., 1999). There is a lack of knowledge on the effect of load level on the time-dependent recovery, and the relative contribution of multiple recovery mechanisms in disc height recovery. Specifically, it remains unknown how increased loading will impact the magnitude, rate, and duration of disc height recovery. In most studies that evaluated disc recovery behavior, a single load condition has been considered, making it difficult to compare findings across studies and generalize observations to different load levels (Bezci and O'Connell, 2018; Castro et al., 2014; Choy and Chan, 2015; Johannessen et al., 2004; O'Connell et al., 2011; Riches et al., 2002; van der Veen et al., 2007; Vresilovic et al., 2006). To further improve the knowledge of load-dependent recovery mechanics, the objective of this study was to quantify unloaded disc recovery behavior after creep loading under a wide range of physiologically relevant stresses.

2. Methods

2.1. Specimen preparation

Bovine caudal discs were used based on similarities to non-degenerate human discs with respect to mechanical and biochemical properties (Beckstein et al., 2008; Bezci et al., 2019, 2018b; Demers et al., 2004; Showalter et al., 2012). Moreover, bovine caudal discs from the upper tail have large disc areas and heights in comparison to other animal discs, making it an attractive animal model for investigating fluid flow and solute diffusion (Alini et al., 2008). Fresh-frozen oxtails were purchased from a local abattoir, and the surrounding musculature was removed with a scalpel (15 spines; age range = 16–18 months). Bone-disc-bone motion segments were prepared from the top two levels of the caudal spine by making parallel cuts through the superior and inferior vertebral bodies with a bone saw (n = 24; levels C1–C3). Vertebral bodies were embedded in polymetheylmethacrylate (PMMA) dental cement to ensure that the loaded surfaces were parallel with the mid-transverse plane of the disc. Each motion segment was wrapped with a saline-soaked gauze (0.15 M phosphate-buffered saline) and stored at -20 °C until testing. Before testing, specimens were hydrated in 0.15 M phosphate-buffered saline at 4 °C for 24 h and then equilibrated to room temperature for 2 h to ensure steady-state hydration levels for all samples.

2.2. Mechanical testing

First, a preliminary study was performed to determine the repeatability of disc recovery behavior, because previous work demonstrated that creep behavior was not repeatable, even after extended recovery (Bass et al., 1997; O'Connell et al., 2011). A nominal compressive preload (10 N) was applied to ensure contact between the specimen and loading platens. Then, each specimen (n = 8) underwent two cycles of creep-recovery loading, where each cycle consisted of a 24-h creep at 1200 N, followed by an 18-h recovery period at 10 N (Fig. 1A). Based on the intradiscal pressure of human lumbar discs, the pressure that corresponds to 10 N may be slightly lower than the pressure experienced during bed rest (i.e., lying supine) (Dreischarf et al., 2016; Wilke et al., 1999). Compression testing was performed at room temperature using a servo-hydraulic material testing system equipped with a saline bath to maintain hydration during testing (Fig. 1A; MiniBionix 858, MTS Systems Corp., Eden Prairie, MN). The saline solution (0.15 M phosphate-buffered saline) was refreshed at the beginning of each creep and recovery period.

Once repeatable recovery behavior was confirmed, disc recovery mechanics were evaluated with respect to the applied compressive stress during creep (n = 16 specimens). A nominal preload (10 N) was applied to ensure contact between the specimen and loading platens. Then, each specimen underwent three cycles of creep-recovery loading, where each cycle consisted of a 24-h creep at a pre-assigned load (100, 200, 300, 600, 900, or 1200 N), followed by an 18-h recovery period at 10 N (Fig. 1B; total testing time = 126 h, loading/unloading rate = 20 N/s). The load applied to each sample was different in each creep period and order of loading was randomized. Changes in disc height were monitored for an extended period of time during unloaded recovery to improve predictions of the equilibrium recovery behavior (Van der Veen et al., 2013). Total testing time was limited to testing times used in previous studies with long-duration test protocols (Korecki et al., 2007; Vergroesen et al., 2018). A wide range of axial compressive loads was selected to represent the wide range of pressures experienced *in vivo* (*e.g.*, lying supine, relaxed standing, and lifting) (Wilke et al., 1999).

2.3. Data analysis

Force and displacement were recorded throughout the test (acquisition rate = 1 Hz). Changes in specimen height (or displacement) during recovery were calculated with respect to the disc height at the end of the previous loading period. Initial recovery rate was calculated from the slope of the time-dependent displacement-time curve using the first 10 min of data. Similarly, the recovery rate at 18 h was calculated by using the slope of the displacement-time curve from the last hour of the testing. Time-dependent recovery behavior was evaluated by curve fitting displacement data to a 5-parameter rheological model, using a

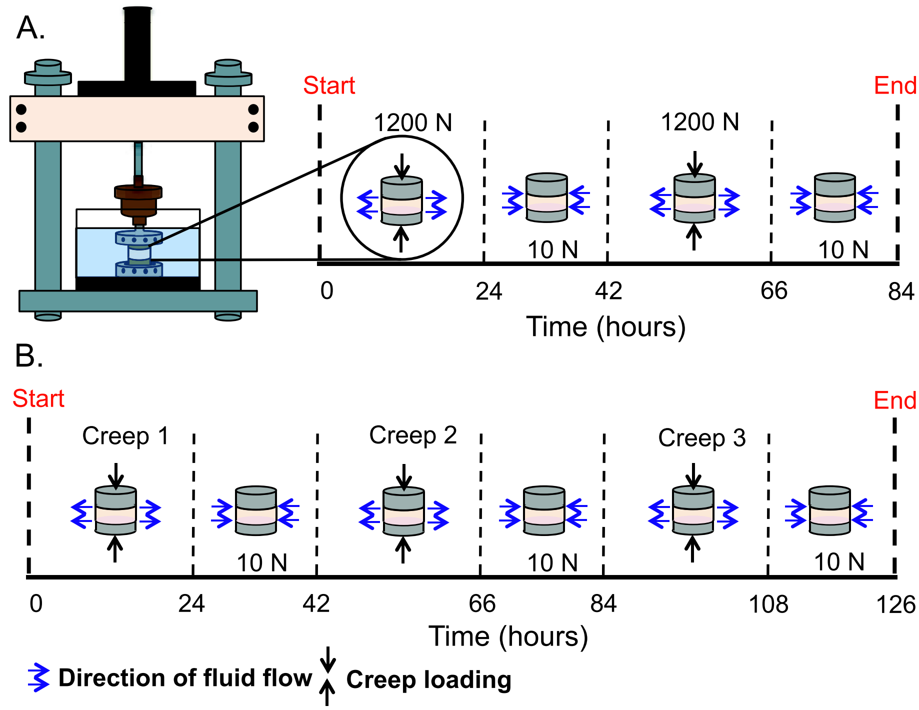

Fig. 1. Schematic of experimental study design to evaluate A) repeatability of recovery behavior and B) load-dependent recovery mechanics. Black arrows indicate compression applied to the motion segment. Blue arrows indicate expected fluid flow during each phase.

non-linear least-squares fitting algorithm (lsqnonlin function, Equation (1); Matlab, Mathworks, Inc., Natick, MA). In Equation (1), parameters τ_1 and τ_2 denote time constants for the fast (or short-term) and slow (or long-term) recovery responses, respectively (Bezci and O'Connell, 2018). Parameters A_1 and A_2 denote asymptotic displacement limits due to fast and slow recovery responses, respectively. To simplify the model, the elastic response parameter, d_E, was assumed to be equal to the displacement measured at the end of the unloading ramp (i.e., displacement at time point, t = Load (N)/20 (N/s)).

$$d = d_E + A_1\left(1 - e^{-\frac{t}{\tau_1}}\right) + A_2\left(1 - e^{-\frac{t}{\tau_2}}\right) \tag{1}$$

The rheological model was used to predict equilibrium displacement (d_{eq}) and equilibrium time (t_{eq}) for recovery. Equilibrium time was calculated as the time when displacement reached 95% of the equilibrium displacement. Individual contributions of elastic, fast, and slow responses to disc recovery behavior were calculated as a percentage of equilibrium displacement (*i.e.*, total recovery response).

After mechanical testing, each motion segment was rehydrated in 0.15 M phosphate-buffered saline for an additional 24 h before removing the disc from the surrounding vertebrae with a scalpel. A digital image of the transverse plane was taken to measure the cross-sectional area (624 ± 57 mm^2). Applied compressive stress was calculated by dividing the applied load by the cross-sectional area.

2.4. Statistics

To assess the repeatability of disc recovery behavior, a paired t-test was used to compare model parameters from the two recovery cycles. The relationship between applied creep stress and recovery model parameters was estimated by fitting each parameter to three functions, including linear, logarithmic, and power functions. The function with the lowest Akaike's Information Criterion (AIC) score was selected for further analyses. The AIC score was used to evaluate goodness-of-fit because the coefficient of determination (R^2) has been shown to be inappropriate for nonlinear models (Spiess and Neumeyer, 2010). When a nonlinear relationship was found, data were log-transformed to convert a nonlinear relationship to a linear one. For linear relationships, the coefficient of determination (R^2) was used to determine the strength of the correlation. R^2 values greater than 0.5 were defined as strong correlations, whereas moderate correlations were assumed for $0.3 \leq R^2 < 0.5$. Any R^2 values less than 0.3 were interpreted as weak correlations.

Mixed effects models were performed to evaluate the statistical significance of applied creep stress and creep-recovery cycle number using the restricted maximum likelihood method. Mixed effects models were chosen to incorporate both random (*i.e.*, specimen information) and fixed variables (*i.e.*, applied load and cycle number). The effect of replicate measurements from each disc and the spine that discs were collected from was evaluated by including disc level and associated animal donor number as nested random variables. All statistical analyses were performed using R software, and significance was assumed for $p < 0.05$.

3. Results

Force-displacement response during creep and recovery was nonlinear (Fig. 2A). Creep behavior reached equilibrium within ~12 h; however, disc height recovery did not reach equilibrium within the 18-h period (slope = 0.59 ± 0.02 mm/h » 0; Fig. 2). The rheological model fit well to data collected during unloaded recovery (Fig. 2B). Model parameters were compared between the two recovery cycles to assess the repeatability of recovery behavior and to ensure that damage did not occur during loading. Unlike the creep response, recovery behavior was highly repeatable with no significant differences in measured elastic and time-dependent displacements or model parameters between the two cycles ($p > 0.48$; Fig. 2A).

For all compressive stresses, the recovery displacement-time curve was highly nonlinear, with a gradually decreasing rate of deformation (Fig. 3A). The initial recovery rate ranged between 0.5 and 2.25 mm/h, and there was a nonlinear relationship between the recovery rate and the applied creep stress (Fig. 3B). After 18 h of recovery, the recovery

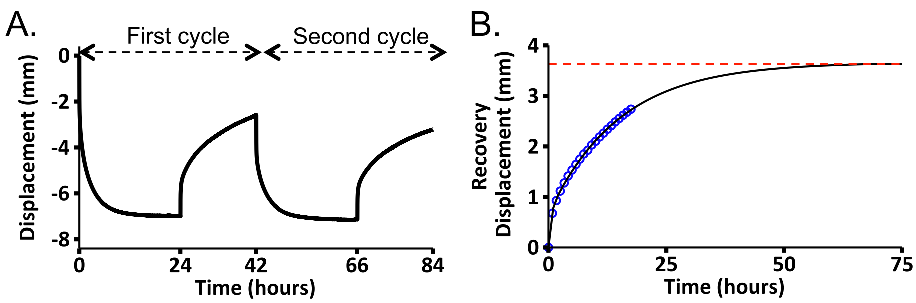

Fig. 2. A) Representative sample showing displacement during two cycles of creep and recovery. B) Representative sample of axial displacement (or disc height) during recovery. Note that displacement was re-zeroed at the beginning of each loading period. Blue circles represent experimental data (every 50th point shown for clarity), the black line represents the model fit, and the dashed red line indicates equilibrium displacement. Recovery was measured for 18 h, because preliminary work showed that a 18-h test was sufficient for predicting equilibrium displacement within 10%.

rate was less than 0.10 mm/h and the 18-h recovery period was insufficient to achieve equilibrium (Fig. 3A & C). There was a nonlinear relationship between the initial displacement during recovery (*i.e.*, elastic recovery displacement) and the applied creep stress (Fig. 3D). Similarly, there was a nonlinear relationship between time-dependent recovery displacement and the applied creep stress (Fig. 3E), resulting in a nonlinear relationship between the equilibrium displacement during recovery and the applied creep stress (Fig. 3F). That is, the difference between recovery curves following 0.5 MPa and 1.0 MPa creep was greater than the difference between recovery curves following 1.5 MPa and 2.0 MPa creep (Fig. 3A). As expected, cycle number did not impact elastic or time-dependent recovery displacements ($p > 0.5$).

The relationship between asymptotic displacement limits for fast and slow recovery responses (*i.e.*, A_1 and A_2, respectively; Equation (1)) and applied creep stress was nonlinear and best described with a logarithmic function ($p < 0.001$; Fig. 4A–B). The magnitude of A_1 was an order of magnitude lower than the magnitude of A_2. In contrast, time constants associated with fast and slow recovery responses did not depend on applied creep stress ($p \geq 0.08$; Fig. 4C–D). The fast time constant was on the order of minutes (range = 10–30 min), while the slow time constant was on the order of hours (range = 8–17 h; Fig. 5C *versus* 5D).

In order to account for differences in recovery displacement due to the applied creep stress, the 5-parameter rheological model was modified to incorporate the applied stress (Equation (2)), where t represents time (seconds) and σ represents applied stress (MPa) during recovery. Model parameters shown in Equation (2) represent average values for all specimens (*i.e.*, the combination of relationships shown in Figs. 3D, 4A and 4B). The modified 5-parameter rheological model well described disc recovery behavior with a single set of model parameters, regardless of applied stress during loading (Fig. 3A – circles versus lines).

$$d = 0.53\sigma^{0.57} + (0.18 ln\,\sigma\ + 0.61)*\left(1 - e^{-\frac{t}{1176}}\right) + (0.45 ln\,\sigma\ + 2.54)*\left(1 - e^{-\frac{t}{43200}}\right) \quad (2)$$

Equilibrium recovery time was 36 ± 7 h and did not depend on applied creep stress ($p = 0.08$). However, the contributions of elastic, fast, and slow recovery responses to the overall equilibrium displacement significantly depended on applied creep stress ($p < 0.01$; Fig. 5A–C). The contribution of the elastic response to the overall equilibrium displacement was strongly correlated with the applied creep stress ($R^2 = 0.66$; Fig. 5A). Similarly, there was a significant, but weak, positive correlation between the contribution of the fast time-dependent response to the overall recovery behavior and applied creep stress ($R^2 = 0.13$; Fig. 5B). Disc height recovery associated with slow time-dependent response accounted for more than 50% of the overall recovery displacement, regardless of the applied creep stress. Moreover, there

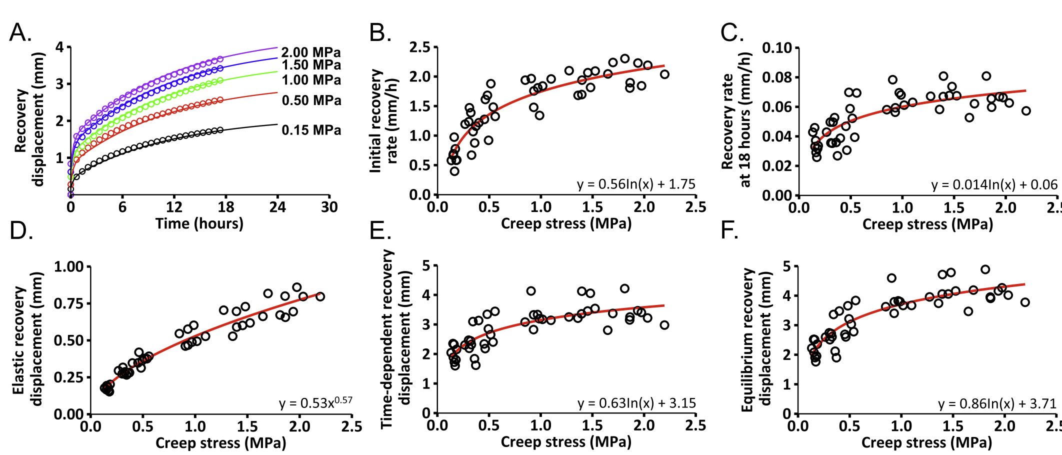

Fig. 3. A) Comparison of experimental recovery data and model predictions for different stress levels. Circles represent experimental data, and curves represent model predictions. Recovery rate at the B) beginning and C) end of the recovery period. Recovery displacement D) measured immediately after unloading (*i.e.* elastic recovery), E) during the length of the recovery period (*i.e.*, time-dependent recovery displacement), and F) predicted recovery displacement at equilibrium. Note that the equilibrium recovery displacement is a summation of the elastic and time-dependent recovery displacements. Circles represent experimental data and red lines indicate nonlinear best-fit lines.

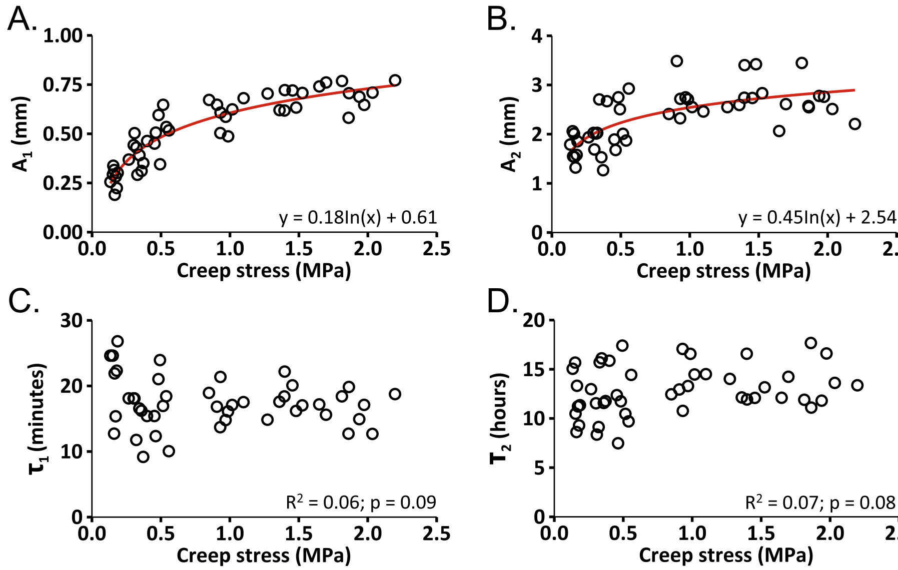

Figure 4. (A–B) Asymptotic limits of displacement due to (A) fast and (B) slow recovery behaviors. (C–D) Time-constants associated with (C) fast and (D) slow recovery behavior. Circles represent experimental data and red lines indicate logarithmic or linear best-fit lines.

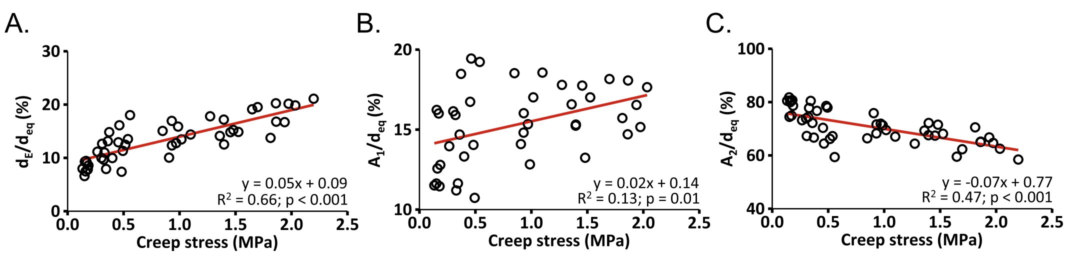

Fig. 5. Percent contribution of (A) elastic, (B) fast, and (C) slow responses to equilibrium recovery displacement. Circles represent experimental data and red lines indicate linear best-fit lines.

was a moderate negative correlation between the contribution of the slow time-dependent response and applied creep stress ($R^2 = 0.47$; Fig. 5C). For low stresses (~0.1 MPa), elastic and fast time-dependent behaviors accounted for ~20% of the overall disc height recovery, whereas slow time-dependent behavior accounted for ~80% of the overall disc height recovery. However, as the applied creep stress increased (~2 MPa), the contribution of elastic and fast time-dependent responses increased to ~35%, while the contribution of slow time-dependent response decreased to ~65%.

4. Discussion

The objective of this study was to characterize the stress-dependent recovery behavior of the intervertebral disc, based on previous observations that noted differences in disc recovery mechanics with loading history (Hwang et al., 2012; O'Connell et al., 2011; Schmidt et al., 2016b; van der Veen et al., 2007). Repeatable measurements of mechanical properties are important for eliminating confounding effects of loading history in studies that employ repeated-measures test protocols. Hence, we first confirmed that the observed recovery behavior was repeatable before evaluating the effect of loading history on recovery mechanics. We found different time-dependent behaviors between the first and second creep cycles, in agreement with previous findings (O'Connell et al., 2011; van der Veen et al., 2008). Despite differences in creep behaviors, identical recovery responses were observed during the two recovery cycles. Similar observations have been reported for ovine and porcine discs subjected to three creep-recovery cycles with shorter loading and recovery periods (*i.e.,* 15 min of loading and 30 min of recovery) (van der Veen et al., 2008, 2007). The discrepancy between creep and recovery repeatability may be due to over-hydration of *in vitro* specimens before testing, resulting in greater fluid flow during the first creep cycle, where fluid flow exchange reaches a steady-state response after the third creep-recovery cycle (Dhillon et al., 2001; Velísková et al., 2018).

The intervertebral disc is a composite material that exhibits both poroelastic and viscoelastic behaviors. Differences in the porosity of the nucleus pulposus and annulus fibrous give rise to anisotropy in ion diffusivity and fluid flow throughout the disc (Gu et al., 2004; Jackson et al., 2006; Sélard et al., 2003; Urban et al., 1977). During compression, much of the initial response is absorbed by water in the tissue. However, over time, compression forces fluid to flow out of the tissue, resulting in pore compaction and additional stress being absorbed by the viscoelastic solid (Chagnon et al., 2010). Dehydration during loading has been observed to cause shrinkage of collagen fibers, which may contribute to time-dependent changes in disc mechanics (Andriotis et al., 2018). In addition, fluid flow out of the disc increases fixed charge density and internal osmotic pressure, causing a pressure gradient with the external environment (Gray et al., 1988). The findings from this study suggest that greater osmotic gradients caused by larger compressive loads result in an increase in fluid flow rate and magnitude during recovery. This finding also agrees with observations of our previous work, where greater disc height recovery was achieved by performing recovery under a hypo-osmotic condition, which increases the osmotic gradient between the disc and surrounding environment (Bezci and O'Connell, 2018).

We used a five-parameter rheological model, consisting of two exponential terms, to characterize the time-dependent disc recovery behavior. As expected, a bi-exponential model provided a better fit to the experimental data than a single exponential model. The choice of using a bi-exponential model was also based on findings from previous studies that identified changes in short-term (minutes) or long-term (hours) disc recovery mechanics with nucleotomy, degeneration, and osmotic loading (Bezci and O'Connell, 2018; O'Connell et al., 2011; Vresilovic et al., 2006). The bi-exponential rheological model with stress-dependent displacement terms was able to accurately describe the apparent time-dependent recovery behavior and provide good predictions of the equilibrium displacement at different stress levels. This observation was in line with our previous work that reported insignificant differences between model predictions from a 12-h recovery test and actual measurements after 48 h of recovery (Bezci and O'Connell, 2018).

Although multiple mechanisms coexist during time-dependent deformation, short-term recovery has been predominantly associated with intrinsic viscoelasticity, rather than fresh fluid being imbibed by the disc through the annulus (Bezci and O'Connell, 2018; Broberg, 1993; O'Connell et al., 2011; van der Veen et al., 2005). In our previous work, altering the external osmotic loading environment only influenced the long-term recovery behavior, where fluid exchange with the surrounding environment is slower than the viscoelastic recovery of the solid matrix or fluid redistribution within the disc (Bezci and O'Connell, 2018). Moreover, previous studies did not observe any increase in nucleus pulposus pressure and fluid content during the first 30 min of recovery (Reitmaier et al., 2012; van der Veen et al., 2005), which is comparable to the time constant of the short-term recovery response reported here. Lastly, tests on desiccated discs showed that creep and recovery were possible without water movement (Koeller et al., 1984), which was further supported by our findings that discs exhibit a nonlinear recovery response in air, without any signs of dehydration over an 18-h recovery period (Fig. S1). Collectively, these findings suggest that recovery response on the order of minutes is largely driven by the viscoelastic response of the solid matrix. In contrast, long-term time-dependent recovery behavior has contributions from both intrinsic viscoelasticity and fluid flow. Although viscoelasticity has a substantial contribution to disc height recovery, fluid flow which is driven by osmotic gradient, is required for disc height and nucleus pressure to be fully restored after overnight bed rest (Emanuel et al., 2018).

Asymptotic displacement limits for short- and long-term recovery responses increased with creep stress, while associated time constants and predicted equilibrium time were insensitive to creep stress. Our finding was in agreement with observations for rat discs, where recovery time constant did not change with creep stress (from 0.5 MPa to 2.0 MPa) (MacLean et al., 2007). However, the initial recovery rate, associated with short-term recovery, was ~4 times greater following compression at 2.0 MPa than compression at 0.1 MPa. The increased rate of initial recovery following larger compressive forces may allow for greater recovery to occur within the same time frame as recovery following low compressive stresses. This finding has potential clinical importance, as it suggests 8 h of bed rest might be sufficient for discs to achieve identical hydration levels, regardless of loading history.

The instantaneous and time-dependent recovery deformations were nonlinearly related to compressive stress, highlighting the nonlinear "viscoelastic" behavior of the intervertebral disc. The nonlinear viscoelastic mechanical behavior was expected based on observations on tendons, ligaments, and vascular tissues (Hingorani et al., 2004; Peña et al., 2011; Provenzano et al., 2001; Troyer and Puttlitz, 2011). Changes in recovery deformation were more pronounced at low compressive stresses, but the increase in recovery deformation diminished after compression at higher stresses (*e.g.*, recovery response following 1 MPa of creep). This complex behavior cannot be comprehensively described by commonly used linear or quasi-linear viscoelastic formulations with constant model parameters. This work showed that a modified five-parameter rheological model with stress-dependent coefficients was adequate for describing recovery behavior following a wide range of compressive stresses (Equation (2)).

The relative contributions of elastic and time-dependent responses to disc height recovery were sensitive to load magnitude. Elastic and fast time-dependent responses represented 20–40% of the total recovery deformation (Fig. 5). However, the relative contribution of the elastic response increased, while the relative contribution of slow time-dependent response decreased linearly with increasing creep stress. This finding suggests that tissue elasticity may become more important for disc height recovery from loading at larger compressive stresses. Increased loading on the spine, such as in professions that require sustained heavy loads (*e.g.,* factory workers or military personnel), might alter disc recovery behavior and limit the convective transfer of nutrients and metabolites necessary for cellular function.

This study is not without its limitations. First, forces exerted by surrounding tissues were neglected and deformations were assumed to be normal to the loading direction. To minimize the additional bending moments during testing, the transverse plane of the disc was positioned parallel to the loading grips and loading was applied at disc center. Second, we chose to use a 5-parameter rheological model to conduct a quantitative assessment of early and late stages of recovery and to make comparisons between tests with different loading magnitudes. However, an ideal constitutive model should describe multiple loading and recovery phenomena with a single set of model parameters. Third, we only investigated recovery behavior under static compression. Physiological loading is more complex, including dynamic and six degrees of freedom loading (Amin et al., 2016; Bezci et al., 2018a). However, previous studies observed similar time-dependent behaviors between dynamic and static loading conditions (Masuoka et al., 2007; van der Veen et al., 2007). Previous work by Masuoka et al. did not observe any significant differences in fluid and height loss of motion segments loaded in compression under cyclic (0.15–1.0 MPa) and static conditions with the same time average magnitudes (0.57 MPa) (Masuoka et al., 2007). Hence, overall trends reported in this study for static loads are expected to be similar to the trends observed for dynamic loads. Lastly, disc mechanics are sensitive to many factors, including loading rate, loading duration, hydration state, spinal level, specimen age, and degeneration (Bezci et al., 2015; Keller et al., 1987; Kemper et al., 2007; Newell et al., 2017; Przybyla et al., 2007). Our study design aimed to minimize the impact of these factors, but differences in test protocols (*e.g.*, loading duration) between this study and previous studies made it difficult to directly compare results, which remains to be a significant challenge in the field (MacLean et al., 2007; van der Veen et al., 2007). This challenge is further heightened with differences in loading path between laboratories and studies; when comparing raw values between labs, data should be corrected for the compliance of the testing machine. However, this study focused on displacements measured during the recovery period, which was observed to have negligible compliance (i.e., no displacement lost in the load train after removing the load). Thus, relative differences between groups during recovery are not affected by compliance during loading.

In conclusion, both short- and long-term time-dependent recovery behaviors strongly depend on the magnitude of applied compression. Instantaneous elastic deformation accounts for 10%–20% of the total disc height recovery, with increasing contribution at larger compressive loads. Both intrinsic viscoelasticity and fluid flow contribute to disc height recovery during low loading periods, such as bed rest. While loading history does not influence the contribution of the short-term recovery, the contribution of long-term recovery is highly sensitive to loading magnitude. Findings from this work, together with previous findings, suggest that short-term recovery is primarily associated with the viscoelastic response of the solid matrix, while long-term recovery response is driven by both intrinsic viscoelasticity and fluid flow due to the osmotic gradient between the disc and surrounding environment. Based on recovery tests in air, approximately 60% of the disc height recovery occurs without water uptake. However, a portion of this recovery might be due to water redistribution from the AF back to the NP. Hence, more complex three-dimensional models and experimental studies are needed to better understand the water uptake and convective transport of solutes during physiological loading.

Declaration of competing interest

The authors certify that there is no conflict of interest related to the work presented in this manuscript.

Acknowledgements

This study was supported by funds from the NSF CAREER Award #1751212.

Appendix A. Supplementary data

Supplementary data to this article can be found online at https://doi.org/10.1016/j.jmbbm.2020.103881.

References

Alini, M., Eisenstein, S.M., Ito, K., Little, C., Kettler, A.A., Masuda, K., Melrose, J., Ralphs, J., Stokes, I., Wilke, H.J., 2008. Are animal models useful for studying human disc disorders/degeneration? Eur. Spine J. https://doi.org/10.1007/s00586-007-0414-y.

Amin, D.B., Lawless, I.M., Sommerfeld, D., Stanley, R.M., Ding, B., Costi, J.J., 2016. The effect of six degree of freedom loading sequence on the in-vitro compressive properties of human lumbar spine segments. J. Biomech. https://doi.org/10.1016/j.jbiomech.2016.09.009.

Andriotis, O.G., Desissaire, S., Thurner, P.J., 2018. Collagen fibrils: nature's highly tunable nonlinear springs. ACS Nano. https://doi.org/10.1021/acsnano.8b00837.

Antoniou, J., Steffen, T., Nelson, F., Winterbottom, N., Hollander, A.P., Poole, R.A., Aebi, M., Alini, M., 1996. The human lumbar intervertebral disc: evidence for changes in the biosynthesis and denaturation of the extracellular matrix with growth, maturation, ageing, and degeneration. J. Clin. Invest. https://doi.org/10.1172/JCI118884.

Argoubi, M., Shirazi-Adl, A., 1996. Poroelastic creep response analysis of a lumbar motion segment in compression. J. Biomech. https://doi.org/10.1016/0021-9290(96)00035-8.

Bass, E.C., Duncan, N.A., Hariharan, J.S., Dusick, J., Ulrich Bueff, H., Lotz, J.C., 1997. Frozen storage affects the compressive creep behaviour of the porcine intervertebral disc. Spine. https://doi.org/10.1097/00007632-199712150-00009. Phila. Pa. 1976.

Beckstein, J.C., Sen, S., Schaer, T.P., Vresilovic, E.J., Elliott, D.M., 2008. Comparison of animal discs used in disc research to human lumbar disc: axial compression mechanics and glycosaminoglycan content. Spine. https://doi.org/10.1097/BRS.0b013e318166e001. Phila. Pa. 1976.

Bezci, S.E., Eleswarapu, A., Klineberg, E.O., O'Connell, G.D., 2018a. Contribution of facet joints, axial compression, and composition to human lumbar disc torsion mechanics. J. Orthop. Res. https://doi.org/10.1002/jor.23870.

Bezci, S.E., Klineberg, E.O., O'Connell, G.D., 2018b. Effects of axial compression and rotation angle on torsional mechanical properties of bovine caudal discs. J. Mech. Behav. Biomed. Mater. https://doi.org/10.1016/j.jmbbm.2017.09.022.

Bezci, S.E., Nandy, A., O'Connell, G.D., 2015. Effect of hydration on healthy intervertebral disk mechanical stiffness. J. Biomech. Eng. https://doi.org/10.1115/1.4031416.

Bezci, S.E., O'Connell, G.D., 2018. Osmotic Pressure Alters Time-dependent Recovery Behavior of the Intervertebral Disc. Spine 43. https://doi.org/10.1097/BRS.0000000000002354. Phila. Pa. 1976.

Bezci, S.E., Werbner, B., Zhou, M., Malollari, K.G., Dorlhiac, G., Carraro, C., Streets, A., O'Connell, G.D., 2019. Radial variation in biochemical composition of the bovine caudal intervertebral disc. JOR Spine. https://doi.org/10.1002/jsp2.1065.

Botsford, D.J., Esses, S.I., Ogilvie-Harris, D.J., 1994. In vivo diurnal variation in intervertebral disc volume and morphology. Spine. https://doi.org/10.1097/00007632-199404150-00012. Phila. Pa. 1976.

Broberg, K.B., 1993. Slow deformation of intervertebral discs. J. Biomech. https://doi.org/10.1016/0021-9290(93)90012-4.

Budday, S., Sommer, G., Holzapfel, G.A., Steinmann, P., Kuhl, E., 2017. Viscoelastic parameter identification of human brain tissue. J. Mech. Behav. Biomed. Mater. https://doi.org/10.1016/j.jmbbm.2017.07.014.

Burns, M.L., Kaleps, I., Kazarian, L.E., 1984. Analysis of compressive creep behavior of the vertebral unit subjected to a uniform axial loading using exact parametric solution equations of Kelvin-solid models-Part I. Human intervertebral joints. J. Biomech. https://doi.org/10.1016/0021-9290(84)90129-5.

Callaghan, J.P., Gunning, J.L., McGill, S.M., 1998. The relationship between lumbar spine load and muscle activity during extensor exercises. Phys. Ther. https://doi.org/10.1093/ptj/78.1.8.

Campana, S., Charpail, E., de Guise, J.A., Rillardon, L., Skalli, W., Mitton, D., 2011. Relationships between viscoelastic properties of lumbar intervertebral disc and degeneration grade assessed by MRI. J. Mech. Behav. Biomed. Mater. https://doi.org/10.1016/j.jmbbm.2011.01.007.

Cassidy, J.J., Silverstein, M.S., Hiltner, A., Baer, E., 1990. A water transport model for the creep response of the intervertebral disc. J. Mater. Sci. Mater. Med. https://doi.org/10.1007/BF00839072.

Castro, A.P.G., Paul, C.P.L., Detiger, S.E.L., Smit, T.H., van Royen, B.J., Pimenta Claro, J.C., Mullender, M.G., Alves, J.L., 2014. Long-term creep behavior of the intervertebral disk: comparison between bioreactor data and numerical results. Front. Bioeng. Biotechnol. https://doi.org/10.3389/fbioe.2014.00056.

Chagnon, A., Aubin, C.É., Villemure, I., 2010. Biomechanical influence of disk properties on the load transfer of healthy and degenerated disks using a poroelastic finite element model. J. Biomech. Eng. https://doi.org/10.1115/1.4002550.

Choy, A.T.H., Chan, B.P., 2015. A structurally and functionally biomimetic biphasic scaffold for intervertebral disc tissue engineering. PLoS One. https://doi.org/10.1371/journal.pone.0131827.

Costi, J.J., Stokes, I.A., Gardner-Morse, M.G., Iatridis, J.C., 2008. Frequency-dependent behavior of the intervertebral disc in response to each of six degree of freedom dynamic loading: solid phase and fluid phase contributions. Spine. https://doi.org/10.1097/BRS.0b013e31817bb116. Phila. Pa. 1976.

Demers, C.N., Antoniou, J., Mwale, F., 2004. Value and limitations of using the bovine tail as a model for the human lumbar spine. Spine. https://doi.org/10.1097/01.brs.0000147744.74215.b0. Phila. Pa. 1976.

Dhillon, N., Bass, E.C., Lotz, J.C., 2001. Effect of frozen storage on the creep behavior of human intervertebral discs. In: Spine. https://doi.org/10.1097/00007632-200104150-00011.

DiSilvestro, M.R., Zhu, Q., Wong, M., Jurvelin, J.S., Suh, J.-K.F., 2001. Biphasic poroviscoelastic simulation of the unconfined compression of articular cartilage: I—simultaneous prediction of reaction force and lateral displacement. J. Biomech. Eng. https://doi.org/10.1115/1.1351890.

Dreischarf, M., Shirazi-Adl, A., Arjmand, N., Rohlmann, A., Schmidt, H., 2016. Estimation of loads on human lumbar spine: a review of in vivo and computational model studies. J. Biomech. https://doi.org/10.1016/j.jbiomech.2015.12.038.

Emanuel, K.S., van der Veen, A.J., Rustenburg, C.M.E., Smit, T.H., Kingma, I., 2018. Osmosis and viscoelasticity both contribute to time-dependent behaviour of the intervertebral disc under compressive load: a caprine in vitro study. J. Biomech. https://doi.org/10.1016/j.jbiomech.2017.10.010.

Ferguson, S.J., Ito, K., Nolte, L.P., 2004. Fluid flow and convective transport of solutes within the intervertebral disc. J. Biomech. https://doi.org/10.1016/S0021-9290(03)00250-1.

Gray, M.L., Pizzanelli, A.M., Grodzinsky, A.J., Lee, R.C., 1988. Mechanical and physicochemical determinants of the chondrocyte biosynthetic response. J. Orthop. Res. https://doi.org/10.1002/jor.1100060602.

Gu, W.Y., Yao, H., Vega, A.L., Flagler, D., 2004. Diffusivity of ions in agarose gels and intervertebral disc: effect of porosity. Ann. Biomed. Eng. https://doi.org/10.1007/s10439-004-7823-4.

Han, K.S., Rohlmann, A., Zander, T., Taylor, W.R., 2013. Lumbar spinal loads vary with body height and weight. Med. Eng. Phys. https://doi.org/10.1016/j.medengphy.2012.09.009.

Hayes, W.C., Bodine, A.J., 1978. Flow-independent viscoelastic properties of articular cartilage matrix. J. Biomech. https://doi.org/10.1016/0021-9290(78)90075-1.

Hingorani, R.V., Provenzano, P.P., Lakes, R.S., Escarcega, A., Vanderby, R., 2004. Nonlinear viscoelasticity in rabbit medial collateral ligament. Ann. Biomed. Eng. https://doi.org/10.1023/B:ABME.0000012751.31686.70.

Hsieh, A.H., Wagner, D.R., Cheng, L.Y., Lotz, J.C., 2005. Dependence of mechanical behavior of the murine tail disc on regional material properties: a parametric finite element study. J. Biomech. Eng. https://doi.org/10.1115/1.2073467.

Hult, E., Ekström, L., Kaigle, A., Holm, S., Hansson, T., 1995. In vivo measurement of spinal column viscoelasticity—an animal model. Proc. Inst. Mech. Eng. Part H J. Eng. Med. https://doi.org/10.1243/PIME_PROC_1995_209_326_02.

Hwang, D., Gabai, A.S., Yu, M., Yew, A.G., Hsieh, A.H., 2012. Role of load history in intervertebral disc mechanics and intradiscal pressure generation. Biomech. Model. Mechanobiol. https://doi.org/10.1007/s10237-011-0295-1.

Iatridis, J.C., MacLean, J.J., O'Brien, M., Stokes, I.A.F., 2007. Measurements of Proteoglycan and Water Content Distribution in Human Lumbar Intervertebral Discs. Spine. https://doi.org/10.1097/BRS.0b013e318067dd3f. Phila. Pa. 1976.

Jackson, A., Yao, H., Brown, M.D., Yong Gu, W., 2006. Anisotropic Ion Diffusivity in Intervertebral Disc: an Electrical Conductivity Approach. Spine. https://doi.org/10.1097/01.brs.0000245842.02717.1b. Phila. Pa. 1976.

Johannessen, W., Vresilovic, E.J., Wright, A.C., Elliott, D.M., 2004. Intervertebral disc mechanics are restored following cyclic loading and unloaded recovery. Ann. Biomed. Eng. https://doi.org/10.1023/B:ABME.0000007792.19071.8c.

Kazarian, L.E., 1975. Creep characteristics of the human spinal column. Orthop. Clin. N. Am.

Keller, T.S., Hansson, T.H., Holm, S.H., Pope, M.M., Spengler, D.M., 1988. In vivo creep behavior of the normal and degenerated porcine intervertebral disk: a preliminary report. J. Spinal Disord.

Keller, T.S., Holm, S.H., Hansson, T.H., Spengler, D.M., 1990. The dependence of intervertebral disc mechanical properties on physiologic conditions. Spine. https://doi.org/10.1097/00007632-199008010-00004. Phila. Pa. 1976.

Keller, T.S., Spengler, D.M., Hansson, T.H., 1987. Mechanical behavior of the human lumbar spine. I. Creep analysis during static compressive loading. J. Orthop. Res. https://doi.org/10.1002/jor.1100050402.

Kelly, T.A.N., Roach, B.L., Weidner, Z.D., Mackenzie-Smith, C.R., O'Connell, G.D., Lima, E.G., Stoker, A.M., Cook, J.L., Ateshian, G.A., Hung, C.T., 2013. Tissue-

engineered articular cartilage exhibits tension-compression nonlinearity reminiscent of the native cartilage. J. Biomech. https://doi.org/10.1016/j.jbiomech.2013.05.017.
Kemper, A.R., McNally, C., Duma, S.M., 2007. The influence of strain rate on the compressive stiffness properties of human lumbar intervertebral discs. In: Biomedical Sciences Instrumentation.
Koeller, W., Funke, F., Hartmann, F., 1984. Biomechanical behavior of human intervertebral discs subjected to long lasting axial loading. Biorheology. https://doi.org/10.3233/BIR-1984-21502.
Korecki, C.L., MacLean, J.J., Iatridis, J.C., 2007. Characterization of an in vitro intervertebral disc organ culture system. Eur. Spine J. https://doi.org/10.1007/s00586-007-0327-9.
Lu, Y.M., Hutton, W.C., 1998. The effect of fluid loss on the viscoelastic behavior of the lumbar intervertebral disc in compression. J. Biomech. Eng. https://doi.org/10.1115/1.2834306.
MacLean, J.J., Owen, J.P., Iatridis, J.C., 2007. Role of endplates in contributing to compression behaviors of motion segments and intervertebral discs. J. Biomech. https://doi.org/10.1016/j.jbiomech.2005.11.013.
Martin, J.T., Gorth, D.J., Beattie, E.E., Harfe, B.D., Smith, L.J., Elliott, D.M., 2013. Needle puncture injury causes acute and long-term mechanical deficiency in a mouse model of intervertebral disc degeneration. J. Orthop. Res. https://doi.org/10.1002/jor.22355.
Martin, J.T., Oldweiler, A.B., Spritzer, C.E., Soher, B.J., Erickson, M.M., Goode, A.P., DeFrate, L.E., 2018. A magnetic resonance imaging framework for quantifying intervertebral disc deformation in vivo: reliability and application to diurnal variations in lumbar disc shape. J. Biomech. https://doi.org/10.1016/j.jbiomech.2018.01.045.
Masuoka, K., Michalek, A.J., MacLean, J.J., Stokes, I.A.F., Iatridis, J.C., 2007. Different effects of static versus cyclic compressive loading on rat intervertebral disc height and water loss in vitro. Spine. https://doi.org/10.1097/BRS.0b013e318133d591. Phila. Pa. 1976.
McMillan, D.W., Garbutt, G., Adams, M.A., 1996. Effect of sustained loading on the water content of intervertebral discs: implications for disc metabolism. Ann. Rheum. Dis. https://doi.org/10.1136/ard.55.12.880.
Nachemson, A.L., 1981. Disc pressure measurements. Spine. https://doi.org/10.1097/00007632-198101000-00020. Phila. Pa. 1976.
Newell, N., Little, J.P., Christou, A., Adams, M.A., Adam, C.J., Masouros, S.D., 2017. Biomechanics of the human intervertebral disc: a review of testing techniques and results. J. Mech. Behav. Biomed. Mater. https://doi.org/10.1016/j.jmbbm.2017.01.037.
O'Connell, G.D., Jacobs, N.T., Sen, S., Vresilovic, E.J., Elliott, D.M., 2011. Axial creep loading and unloaded recovery of the human intervertebral disc and the effect of degeneration. J. Mech. Behav. Biomed. Mater. https://doi.org/10.1016/j.jmbbm.2011.02.002.
O'Connell, G.D., Vresilovic, E.J., Elliott, D.M., 2007. Comparison of animals used in disc research to human lumbar disc geometry. Spine. https://doi.org/10.1097/01.brs.0000253961.40910.c1. Phila. Pa. 1976.
Oftadeh, R., Connizzo, B.K., Nia, H.T., Ortiz, C., Grodzinsky, A.J., 2018. Biological connective tissues exhibit viscoelastic and poroelastic behavior at different frequency regimes: application to tendon and skin biophysics. Acta Biomater. https://doi.org/10.1016/j.actbio.2018.01.041.
Peña, J.A., Martínez, M.A., Peña, E., 2011. A formulation to model the nonlinear viscoelastic properties of the vascular tissue. Acta Mech. https://doi.org/10.1007/s00707-010-0378-6.
Pollintine, P., Van Tunen, M.S.L.M., Luo, J., Brown, M.D., Dolan, P., Adams, M.A., 2010. Time-dependent compressive deformation of the ageing spine: relevance to spinal stenosis. Spine. https://doi.org/10.1097/BRS.0b013e3181b0ef26. Phila. Pa. 1976.
Provenzano, P., Lakes, R., Keenan, T., Vanderby, R., 2001. Nonlinear ligament viscoelasticity. Ann. Biomed. Eng. https://doi.org/10.1114/1.1408926.
Przybyla, A.S., Skrzypiec, D., Pollintine, P., Dolan, P., Adams, M.A., 2007. Strength of the cervical spine in compression and bending. Spine. https://doi.org/10.1097/BRS.0b013e318074c40b. Phila. Pa. 1976.
Reitmaier, S., Shirazi-Adl, A., Bashkuev, M., Wilke, H.J., Gloria, A., Schmidt, H., 2012. In vitro and in silico investigations of disc nucleus replacement. J. R. Soc. Interface. https://doi.org/10.1098/rsif.2012.0016.
Riches, P.E., Dhillon, N., Lotz, J., Woods, A.W., McNally, D.S., 2002. The internal mechanics of the intervertebral disc under cyclic loading. J. Biomech. https://doi.org/10.1016/S0021-9290(02)00070-2.
Schmidt, H., Schilling, C., Reyna, A.L.P., Shirazi-Adl, A., Dreischarf, M., 2016a. Fluid-flow dependent response of intervertebral discs under cyclic loading: on the role of specimen preparation and preconditioning. J. Biomech. https://doi.org/10.1016/j.jbiomech.2015.10.029.
Schmidt, H., Shirazi-Adl, A., Schilling, C., Dreischarf, M., 2016b. Preload substantially influences the intervertebral disc stiffness in loading-unloading cycles of compression. J. Biomech. https://doi.org/10.1016/j.jbiomech.2016.05.006.
Sélard, E., Shirazi Adl, A., Urban, J.P.G., 2003. Finite element study of nutrient diffusion in the human intervertebral disc. Spine. https://doi.org/10.1097/01.BRS.0000087210.93541.23. Phila. Pa. 1976.
Showalter, B.L., Beckstein, J.C., Martin, J.T., Beattie, E.E., Orías, A.A.E., Schaer, T.P., Vresilovic, E.J., Elliott, D.M., 2012. Comparison of animal discs used in disc research to human lumbar disc: torsion mechanics and collagen content. Spine. https://doi.org/10.1097/BRS.0b013e31824d911c. Phila. Pa. 1976.
Spiess, A.N., Neumeyer, N., 2010. An evaluation of R2as an inadequate measure for nonlinear models in pharmacological and biochemical research: a Monte Carlo approach. BMC Pharmacol. https://doi.org/10.1186/1471-2210-10-6.
Suh, J.K., Disilvestro, M.R., 1999. Biphasic poroviscoelastic behavior of hydrated biological soft tissue. J. Appl. Mech. Trans. ASME. https://doi.org/10.1115/1.2791079.
Troyer, K.L., Puttlitz, C.M., 2011. Human cervical spine ligaments exhibit fully nonlinear viscoelastic behavior. Acta Biomater. https://doi.org/10.1016/j.actbio.2010.09.003.
Urban, J.P.G., Holm, S., Maroudas, A., Nachemson, A., 1982. Nutrition of the intervertebral disc. Effect of fluid flow on solute transport. Clin. Orthop. Relat. Res. https://doi.org/10.1097/00003086-198210000-00039.
Urban, J.P.G., Holm, S., Maroudas, A., Nachemson, A., 1977. Nutrition of the intervertebral disk. An in vivo study of solute transport. Clin. Orthop. Relat. Res. https://doi.org/10.1097/00003086-197711000-00012.
Van der Veen, A.J., Bisschop, A., Mullender, M.G., van Dieën, J.H., 2013. Modelling creep behaviour of the human intervertebral disc. J. Biomech. https://doi.org/10.1016/j.jbiomech.2013.05.026.
van der Veen, A.J., Mullender, M., Smit, T.H., Kingma, I., van Dieën, J.H., 2005. Flow-related mechanics of the intervertebral disc: the validity of an in vitro model. Spine. https://doi.org/10.1097/01.brs.0000179306.40309.3a. Phila. Pa. 1976.
van der Veen, A.J., Mullender, M.G., Kingma, I., van, J.H., Smit, T.H., 2008. Contribution of vertebral bodies, endplates, and intervertebral discs to the compression creep of spinal motion segments. J. Biomech. https://doi.org/10.1016/j.jbiomech.2008.01.010.
van der Veen, A.J., van Dieën, J.H., Nadort, A., Stam, B., Smit, T.H., 2007. Intervertebral disc recovery after dynamic or static loading in vitro: is there a role for the endplate? J. Biomech. https://doi.org/10.1016/j.jbiomech.2006.10.018.
Velísková, P., Bashkuev, M., Shirazi-Adl, A., Schmidt, H., 2018. Computational study of the role of fluid content and flow on the lumbar disc response in cyclic compression: replication of in vitro and in vivo conditions. J. Biomech. https://doi.org/10.1016/j.jbiomech.2017.10.032.
Vergroesen, P.P.A., Emanuel, K.S., Peeters, M., Kingma, I., Smit, T.H., 2018. Are axial intervertebral disc biomechanics determined by osmosis? J. Biomech. https://doi.org/10.1016/j.jbiomech.2017.04.027.
Vergroesen, P.P.A., van der Veen, A.J., Emanuel, K.S., van Dieën, J.H., Smit, T.H., 2016. The poro-elastic behaviour of the intervertebral disc: a new perspective on diurnal fluid flow. J. Biomech. https://doi.org/10.1016/j.jbiomech.2015.11.041.
Vergroesen, P.P.A., Van Der Veen, A.J., Van Royen, B.J., Kingma, I., Smit, T.H., 2014. Intradiscal pressure depends on recent loading and correlates with disc height and compressive stiffness. Eur. Spine J. https://doi.org/10.1007/s00586-014-3450-4.
Vresilovic, E.J., Johannessen, W., Elliott, D.M., 2006. Disc mechanics with trans-endplate partial nucleotomy are not fully restored following cyclic compressive loading and unloaded recovery. J. Biomech. Eng. https://doi.org/10.1115/1.2354210.
Wilke, H.J., Neef, P., Caimi, M., Hoogland, T., Claes, L.E., 1999. New in vivo measurements of pressures in the intervertebral disc in daily life. Spine. https://doi.org/10.1097/00007632-199904150-00005. Phila. Pa. 1976.
Xu, B., Li, H., Zhang, Y., 2013. Understanding the viscoelastic behavior of collagen matrices through relaxation time distribution spectrum. Biomatter. https://doi.org/10.4161/biom.24651.
Zhu, W., Mow, V.C., Koob, T.J., Eyre, D.R., 1993. Viscoelastic shear properties of articular cartilage and the effects of glycosidase treatments. J. Orthop. Res. https://doi.org/10.1002/jor.1100110602.